Structural origin underlying the effect of cooling rate on solidification point*

Li Chen-Hui(李晨辉), Han Xiu-Jun(韩秀君)†, Luan Ying-Wei(栾英伟), and Li Jian-Guo(李建国)

Laboratory of Advanced Materials Solidification, School of Materials Science and Engineering, Shanghai Jiao Tong University, Shanghai 200240, *China*

(Received 3 May 2015; revised manuscript received 15 July 2015; published online 12 October 2015)

Solidification behaviors of liquid aluminum at different cooling rates were examined via classical molecular dynamics simulation with an embedded atom method potential. The results demonstrate that solidification point decreases with increasing cooling rate. To explain this phenomenon, solid-like cluster in liquid was analyzed by the structural analysis method of bond order parameters. The results reveal that the size of the largest solid-like cluster in deeply undercooled liquid decreases with the increase of cooling rate, which can provide a structural interpretation to the above phenomenon.

Keywords: liquid metal, undercooled solidification, local structure, molecular dynamics

PACS: 61.25.Mv, 64.70.D–, 61.20.Ja **DOI:** 10.1088/1674-1056/24/11/116101

1. Introduction

Solidification of liquid metal is a fundamental issue in material sciences since almost all kinds of metals we used have to undergo such a procedure at least once or more.[1] In experiments, solidification process is always influenced by impurity, even advanced levitation techniques are employed,[2,3] which hinders our further understanding of the fundamental principle of solidification. To overcome the experimental problem, molecular dynamics (MD) simulation has been widely used since the problem of impurity does not exist. MD simulation is a powerful tool to explore the phase transformation and structure of condensed matter at the level of atomic resolution.[4] In MD simulation, aluminum (Al) is often selected as a model metal for investigation[5–8] due to the wide application of Al as a good engineering material. For example, Shen *et al.*[9] recently presented different solidification processes of liquid Al with the respective cooling rate, and they found that the high cooling rate leads to glass formation, while the low cooling rate leads to crystallization.

As we know, the cooling rate is an important factor during a solidification process, and has a profound effect on the final structures.[10,11] However, the dependence of solidification behavior on cooling rate is still poorly understood. Shibuta *et al.*[12] investigated the effect of cooling rate on the solidification behavior of molybdenum nanoparticle, and they observed that the solidification point decreases with increasing cooling rate. A similar observation was found in bulk nanocrystalline Al.[13] These studies provide us with a deeper knowledge of solidification behavior, but one question coming is why the solidification point decreases with increasing cooling rate. It is well known that, solidification process stems from nucleation except glass transition. Kelton *et al.*[14] demonstrated that a correlation exists between nucleation barrier and icosahedral short-range order, which is a kind of liquid local structure. Inspired by their work, we think that the decrease of solidification point with increasing cooling rate might be associated with liquid local structure. Recently, liquid local structure has attracted great attention both in experiments[15–18] and in MD simulations,[19,20] showing more and more importance in material science. Therefore, in this work, we try to provide an explanation to the above question from the view of liquid local structure.

Firstly, the solidification of liquid Al is conducted using MD simulation with different cooling rate. The cooling rates we selected differ by an order of magnitude, allowing us to clearly observe the discrepancy caused by cooling rate. Secondly, solidification point at each cooling rate is summarized. At last, we present the result of liquid local structure. Based on the result and the classical nucleation theory,[1] the correlation between cooling rate and solidification point is well interpreted. Much attention has been directed to the study of the equilibrium liquid structure, while the liquid structure during a non-equilibrium process like solidification has been rarely reported. We believe this work could attract more attention to further explore the liquid structure at non-equilibrium states.

*Project supported by the National Basic Research Program of China (Grant No. 2011CB012900), the National Natural Science Foundation of China (Grant No. 51171115), the Natural Science Foundation of Shanghai City, China (Grant No. 10ZR1415700), the Research Fund for the Doctoral Program of Higher Education of China (Grant No. 20100073120008), the Program for New Century Excellent Talents in Universities of China. This work is partially supported by Alexander von Humboldt Foundation.

†Corresponding author. E-mail: xjhan@sjtu.edu.cn

© 2015 Chinese Physical Society and IOP Publishing Ltd

2. Simulation details

All simulations were performed under external constant pressure of zero using the open source code LAMMPS.[21] The Finnis–Sinclair potential was adopted to describe the atomic interactions. The original file of the potential for Al is provided by Mendelev.[22] The potential has already been applied to predict the solidification and devitrification of Al.[23] Within the framework of embedded atom method, the total energy $E_{\rm tot}$ consists of two terms

$$E_{\rm tot} = \sum_{i=1}^{N-1} \sum_{j=i+1}^{N} \phi_{ij}(r_{ij}) + \sum_{i=1}^{N} F_i(\rho_i), \tag{1}$$

where i, j denote different atoms, N the number of atoms, r_{ij} the distance between atoms i and j, $\varphi_{ij}(r_{ij})$ the pair potential between atom i and j at a distance of r_{ij}, $F_i(\rho_i)$ the embedded energy, and ρ_i the background charge density at the site of atom i

$$\rho_i = \sum_j \psi_i(r_{ij}), \tag{2}$$

with $\psi_i(r_{ij})$ being the contribution to the charge density at atom i due to atom j.

The system size ($8.1 \times 8.1 \times 8.1$ nm with 32000 atoms) we used in simulation is large enough to observe the liquid-solid transition and exhibit negligible size effect of results. During simulations, periodical boundary conditions (PBCs) are used in three directions. Isothermal-isobaric ensemble (NPT) was used and controlled by the Nosé–Hoover method.[24,25] A time step of 1 fs was applied with Verlet algorithm[26] to integrate Newton's equation of motions. The solidification of liquid Al was performed as follows. Firstly, the whole system was heated up to 2050 K, much higher than the experimental melting point (933.47 K), and held there for 600000 steps to make sure that the system is in complete liquid state. Then, the system was cooled linearly in time from 2050 to 50 K at the cooling rate ranging from 2.0×10^{10} to 2.0×10^{13} K/s, i.e., $T(t) = T_0 - Qt$, where Q is the cooling rate. Each cooling process was repeated 3 times. At each desired temperature, the configuration was recorded for further analysis. Table 1 lists the cooling rates and the corresponding numbers of steps.

Table 1. Cooling rates and correponding numbers of steps.

Q	Cooling rate/K·s^{-1}	Number of steps
Q_1	2.0×10^{10}	1.0×10^{8}
Q_2	2.0×10^{11}	1.0×10^{7}
Q_3	2.0×10^{12}	1.0×10^{6}
Q_4	2.0×10^{13}	1.0×10^{5}

3. Results and discussion

Figure 1 shows the evolution of the total energy per atom (E) with decreasing temperature at the four cooling rates. At Q_1, Q_2, and Q_3, there is an abrupt change of the linear temperature dependence of E, which means liquid Al crystallizes during the cooling. It is observed that, within the transition region, E drops sharply at Q_1 and Q_2, while smoothly at Q_3. This means that the nulceation resistance becomes significantly higher at Q_3 than that at Q_1 and Q_2. For Q_1, Q_2, and Q_3, we define the solidification point as the temperature where the linear decrease in E–T curve disappears. It is seen that the solidification points at the three cooling rates are all far lower than the simulated melting temperature ($T_{\rm m}$), $T_{\rm m} = 912.5$ K. The simulation details of $T_{\rm m}$ are illustrated in Appendix A. At Q_4, E decreases continuously within the whole temperature range, and no abrupt change can be observed, which is a typical feature of glass transition. The glass transition temperature ($T_{\rm g}$) is 350 K, which is determined by the Wendt–Abraham parameter[27] (seen Appendix B). For Q_4, $T_{\rm g}$ is considered as the solidification point. From Fig. 1, we can conclude that the solidification point decreases with increasing cooling rate, which is consistent with the result of Ref. [12].

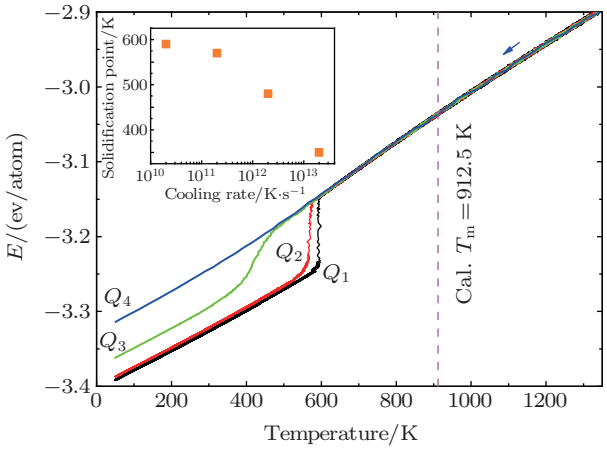


Fig. 1. (color online) E–T curves under various cooling rates. The inset is the summarized solidification point.

There is now a general consensus that liquid metals are composed of various kinds of local structure.[15–20] One important kind of local structure is the solid-like cluster which is generated by liquid structure fluctuation. Solid-like cluster is directly related to the solidification process because one proper solid-like cluster in liquid, especially in deeply undercooled liquid, is enough to initiate nucleation and induce crystallization. In order to further examine the potential mechanism underlying the correlation between cooling rate and solidification point, we have calculated the maximum size of solid-like cluster at different temperature in liquid using the recorded configurations. To do this, we determine the solid-like cluster by using the method of bond-order parameters.[28,29] The advantage of this method is that it can efficiently distinguish solid-like and liquid-like atoms and has little relation to specific type

of crystal. This method has been successfully applied in previous studies by other researchers.[30,31] For each atom i, the normalized order parameter is defined as

$$\hat{q}_{lm}(i) = \frac{1}{AB(i)} \sum_{j=1}^{B(i)} Y_{lm}(\hat{r}_{ij}), \tag{3}$$

where A is a normalization factor, $B(i)$ the number of neighbors of atom i, Y_{lm} a spherical harmonic function, and $\hat{r}_{ij}$ the unit vector pointing from atom i to j. If the complex inner product $\sum_m \hat{q}_{lm}(i)\hat{q}^*_{lm}(j)$ is larger than 0.5, the neighboring atoms i and j are deemed to be ordered neighbors. On the basis of predecessor's work and the usual convention, atoms with more than 8 ordered neighbors (including 8) are identified as solid-like.[32] If an atom has less than 8 ordered neighbors, it is considered to be liquid-like. The validity of the criterion is demonstrated in Ref. [33]. Using this criterion, solid-like cluster formed by adjacent solid-like atoms can be well located. The size of the largest solid-like cluster, N_{MAX}, as a function of temperature is presented in Fig. 2. The temperature range we focus on is from 650 to 1050 K, because no solid-like cluster is found at a temperature higher than 1050 K, while the impending nucleation is detrimental to the reasonability of the information we care about at temperatures lower than 650 K. The first minimum of pair distribution function $g(r)$ is used as a cutoff distance for the determination of solid-like cluster. As shown in Fig. 2, solid-like clusters have already existed in superheated liquid. Solid-like cluster first appears under Q_1 as temperature decreases. Obviously, the probability of finding solid-like clusters in undercooled liquid is much larger than that in superheated liquid. N_{MAX} shows a general trend of increasing with the decrease of temperature, and increases rapidly when the temperature is close to crystallization. The change of N_{MAX} with temperature can be approximated by an exponential expression, and the fitted results are presented in the small inserted figure. It is observed that, at Q_1, Q_2, and Q_3, N_{MAX} grows with decreasing temperature by orders of magnitude over a narrow temperature range near crystallization, and the growth rate becomes higher if the liquid is cooled with a slower cooling rate. At 650 K, N_{MAX} in the undercooled liquid has a clear difference among the four cooling rates, and the slower cooling rate produces the larger N_{MAX}. This observation may uncover why a slower cooling rate causes a higher solidification point. According to the classical nucleation theory, the Gibbs free energy difference ΔG to form a spherical nucleus in undercooled liquid consists of a volume term and an interfacial term,

$$\Delta G = \frac{4}{3}\pi r^3 \Delta G_{\mathrm{V}} + 4\pi r^2 \sigma_{\mathrm{sl}}, \tag{4}$$

where r is the nucleus radius, σ_{sl} the solid/liquid interfacial energy, and ΔG_{V} the volumetric free energy change. The maximum ΔG marked as ΔG^* is received at a critical radius r^*

$$\Delta G^* = \frac{16\pi\sigma_{sl}^3}{3\Delta G_{\mathrm{V}}^2},$$
$$r^* = -\frac{2\sigma_{sl}}{\Delta G_{\mathrm{V}}}. \tag{5}$$

If the size of solid-like cluster is smaller than r^*, the cluster will dissolve. Otherwise, it will grow further and induce crystallization. From Fig. 2, it is most probable for Q_1 to firstly form a solid-like cluster with a radius larger than r^*. That is to say, it is easier for the liquid to firstly crystallize at Q_1 than at the other three cooling rates, and consequently the solidification point at Q_1 will be higher than that at Q_2 and Q_3. The similar discussion can be applied to Q_2 and Q_3, which can well explain why the solidification point decreases with increasing cooling rate. If the cooling rate (like Q_4) is high enough to exceed the critical glass transition cooling rate, the solidification process is a glass transition rather than crystallization. Then the solidification point should be T_{g} which is considerably lower than the crystallization temperature. Because the solidification mechanism has changed, here we limit our discussion to the crystallization.

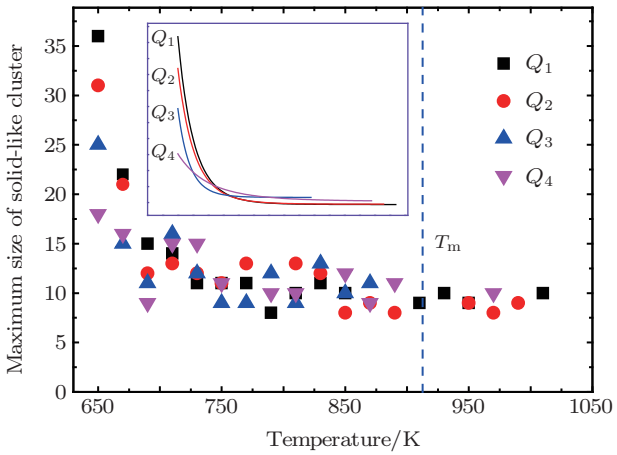


Fig. 2. (color online) The maximum size of solid-like cluster as a function of temperature. The inset is the fitting line. The size of solid-like cluster is characterized by the number of atoms it contains.

4. Conclusions

In summary, a series of MD simulations were performed to examine the cooling rate effect on the solidification behavior of liquid Al. The observed solidification points are all far lower than the simulated melting point, which indicates that the solidifications at the four cooling rates need a quite large undercooling. At the cooling rate less than or equal to 2.0×10^{12} K/s, crystallization takes place. At the cooling rate of 2.0×10^{13} K/s, glass transition is obtained and the corresponding glass transition temperature is 350 K. Following the increase of cooling rate, there is a clear drop of the solidification point. In order to elucidate that, solid-like clusters in undercooled and superheated liquid were analyzed. The results

suggest that, within the temperature range near crystallization, the maximum size of solid-like cluster diminishes remarkably if the cooling rate increases a lot. This observation combined with the classical nucleation theory can reveal the structural origin underlying the effect of cooling rate on solidification point.

Appendix A: Simulation details of predicting the melting temperature with the present potential

In order to determine T_m, a metastable liquid–solid coexisting (sandwich) structure was established, as shown in Fig. A1. The sandwich structure was applied successfully to determine T_m of Au–Cu[34] and Cu–Zr[35] alloys. The simulation box (4.05 × 4.05 × 16.2 nm subject to PBCs in three dimensions) contains 16000 atoms, and is equally divided into two parts, namely, the liquid zone and the solid zone. The liquid zone containing 8000 atoms is in the middle. The solid zone is on the sides of the liquid zone, and also has 8000 atoms. All the atoms are equilibrated at 200 K for 50000 steps. Then the middle part is heated up to 1600 K, and held there for 500000 steps to obtain liquid state. During simulations, the NPT ensemble is used with zero external pressure. The initial configuration is illustrated in Fig. A1. Then the whole system is annealed at different external temperatures for 600000 steps to evolve into an equilibrium end state. Through calculating the average total energy per atom (E) at different end states, T_m can be determined. The result is presented in Fig. A2. It is obvious that E increases as the aging temperature increases. A critial temperature is defined as T_m, where a discontinuous evolution in E–T curve takes place. For a more common method to determine T_m, the molar specific heats (C_p) at different temperatures are calculated from the differential of the enthalpy: $C_p = \mathrm{d}H(T)/\mathrm{d}T$. T_m can also be well determined by the jump in C_p–T curve. As shown in Fig. A3, the configuration crystallizes at 912 K, while it becomes liquid state at 913 K. Therefore, the average value 912.5 K is taken as T_m. The simulated melting point agrees quite well with the experimental value, the deviation being −2.25%.

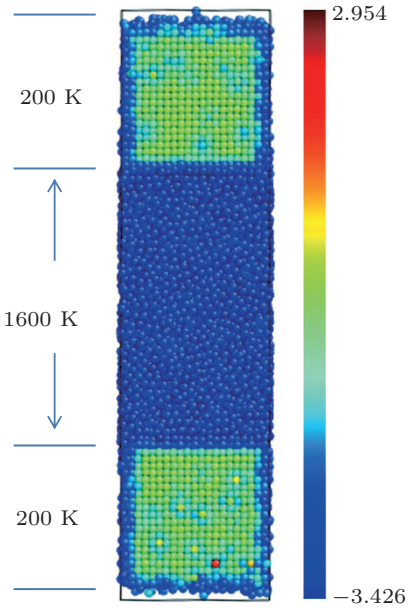


Fig. A1. (color online) Snapshot of the liquid–solid coexisting structure. The colormap denotes potential energy.

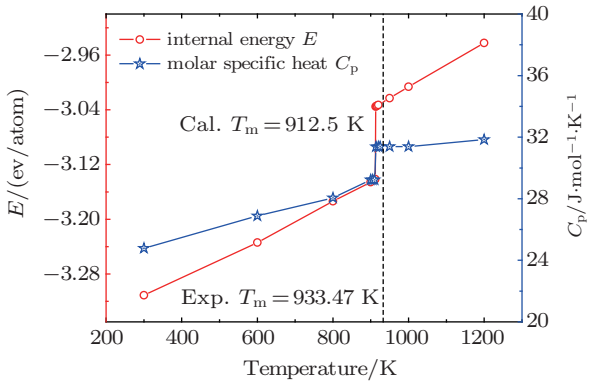


Fig. A2. (color online) Total energy per atom and molar specific heat at the end state of the coexisting structure annealed at different temperatures.

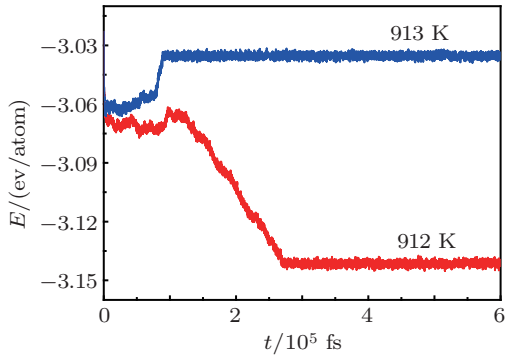


Fig. A3. (color online) Variation of the instantaneous total energy per atom of the coexisting structure at annealing temperatures of 912 and 913 K.

Appendix B: Details of determining glass transition temperature at Q_4

The Wendt–Abraham parameter[27] is for determining glass transition temperature T_g, which is defined as the ratio between the first minimum and maximum of $g(r)$ (g_{min}/g_{max}). Temperature dependence of g_{min}/g_{max} can be treated as two distinct linear regions with the respective characteristic slope. The intersection of the two lines yields a T_g of 350 K, which is illustrated in Fig. B1. The original data for $g(r)$ is shown in Fig. B2.

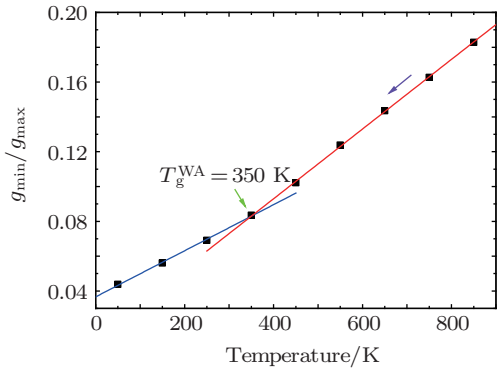


Fig. B1. (color online) Determination of T_g under cooling rate Q_4.

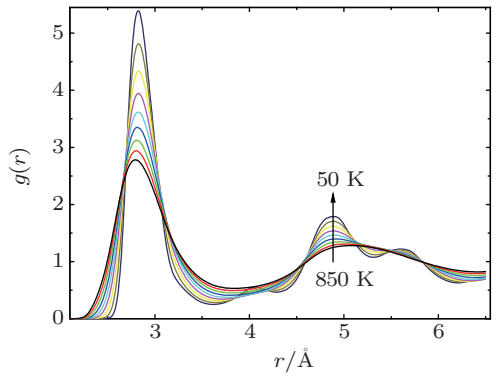


Fig. B2. (color online) Pair distribution function for Al at different temperatures (from low to top, the temperature changes from 850 to 50 K with a step of 100 K).

References

[1] Kurz W and Fisher D J 1986 *Fundamentals of Solidification*, 1984 edition (Switzerland: Trans. Tech. Publications LTD)

[2] Notthoff C, Feuerbacher B, Franz H, Herlach D M and Holland-Moritz D 2001 *Phys. Rev. Lett.* **86** 1038

[3] Willnecker R, Herlach D M and Feuerbacher B 1986 *Appl. Phys. Lett.* **49** 1339

[4] Rapaport D C 2004 *The Art of Molecular Dynamics Simulation,* 2004 edition (Cambridge: Cambridge University Press)

[5] Kramer M J, Mendelev M I and Asta M 2014 *Philos. Mag.* **94** 1876

[6] Li F, Liu X J, Hou H Y, Chen G and Chen G L 2011 *J. Appl. Phys.* **110** 013519

[7] Mendelev M I, Schmalian J, Wang C Z, Morris J R and Ho K M 2006 *Phys. Rev. B* **74** 104206

[8] Li M Z, Wang C Z, Mendelev M I and Ho K M 2008 *Phys. Rev. B* **77** 184202

[9] Shen B, Liu C Y, Jia Y, Yue G Q, Ke F S, Zhao H B, Chen L Y, Wang S Y, Wang C Z and Ho K M 2014 *J. Non-cryst. Solids* **383** 13

[10] Xia J C, Zhu Z G and Liu C S 1999 *Chin. Phys. Lett.* **16** 850

[11] Liu C S, Zhu Z G, Xia J C and Sun D Y 2000 *Chin. Phys. Lett.* **17** 34

[12] Shibuta Y and Suzuki T 2011 *Chem. Phys. Lett.* **502** 82

[13] Hou Z Y, Tian Z, Mo Y F and Liu R S 2014 *Comp. Mater. Sci.* **92** 199

[14] Kelton K F, Lee G W, Gangopadhyay A K, Hyers R W, Rathz T J, Rogers J R, Robinson M B and Robinson D S 2003 *Phys. Rev. Lett.* **90** 195504

[15] Mauro N A, Bendert J C, Vogt A J, Gewin J M and Kelton K F 2011 *J. Chem. Phys.* **135** 044502

[16] Hirata A, Guan P F, Fujita T, Hirotsu Y, Inoue A, Yavari A R, Sakurai T and Chen M W 2011 *Nat. Mater.* **10** 28

[17] Di Cicco A, Iesari F, De Panfili S, Celino M, Giusepponi S and Filipponi A 2014 *Phys. Rev. B* **89** 060102

[18] Mauro N A, Wessels V, Bendert J C, Klein S, Gangopadhyay A K, Kramer M J, Hao S G, Rustan G E, Kreyssig A, Goldman A I and Kelton K F 2011 *Phys. Rev. B* **83** 184109

[19] Ding J, Cheng Y Q and Ma E 2014 *Acta Mater.* **69** 343

[20] Xiong L H, Lou H B, Wang X D, Debela T T, Cao Q P, Zhang D X, Wang S Y, Wang C Z and Jiang J Z 2014 *Acta Mater.* **68** 1

[21] http://lammps.sandia.gov/

[22] Mendelev M I, Kramer M J, Becker C A and Asta M 2008 *Philos. Mag.* **88** 1723

[23] Mendelev M I 2012 *Modelling Simul. Mater. Sci. Eng.* **20** 045014

[24] Nosé S 1984 *J. Chem. Phys.* **81** 511

[25] Hoover W G 1985 *Phys. Rev. A* **31** 1695

[26] Verlet L 1967 *Phys. Rev.* **159** 98

[27] Wendt H R and Abraham F F 1978 *Phys. Rev. Lett.* **41** 1244

[28] Steinhardt P J, Nelson D R and Ronchetti M 1983 *Phys. Rev. B* **28** 784

[29] ten Wolde P N, Ruiz-Montero M J and Frenkel D 1996 *J. Chem. Phys.* **104** 9932

[30] Dullens R P A, Aarts D G A L and Kegel W K 2006 *Phys. Rev. Lett.* **97** 228301

[31] Gasser U, Weeks E R, Schofield A, Pusey P N and Weitz D A 2001 *Science* **292** 258

[32] Guzmán J H and Weeks E R 2009 *Proc. Nati. Acad. Sci. USA* **106** 15198

[33] Lechner W and Dellago C 2008 *J. Chem. Phys.* **129** 114707

[34] Han X J, Chen M and Guo Z Y 2004 *J. Phys.: Condens. Matter* **16** 705

[35] Han X J and Schober H R 2011 *Phys. Rev. B* **83** 224201